

## POSTER ABSTRACTS

### **A QM/MM equation-of-motion coupled-cluster approach for predicting semiconductor color-center structure and emission frequencies**

*J.J. Lutz<sup>1</sup>, X.F. Duan<sup>2</sup>, and L.W. Burggraf<sup>1</sup>*

<sup>1</sup>Air Force Institute of Technology, Wright-Patterson Air Force Base

<sup>2</sup>Air Force Research Laboratory DoD Supercomputing Resource Center, Wright-Patterson Air Force Base

Valence excitation spectra were computed for deep-center silicon-vacancy defects in 3C, 4H, and 6H silicon carbide (SiC) and comparisons were made with literature photoluminescence measurements. Optimizations of nuclear geometries surrounding the defect centers were performed within a Gaussian basis-set framework using many-body perturbation theory or density functional theory (DFT) methods, with computational expenses minimized by a QM/MM technique called SIMOMM. Vertical excitation energies were subsequently obtained by applying excitation-energy, electron- attached, and ionized equation-of-motion coupled-cluster (EOMCC) methods, where appropriate, as well as time-dependent (TD) DFT, to small models including only a few atoms adjacent to the defect center. We consider the relative quality of various EOMCC and TD-DFT methods for (i) energy-ordering potential ground states differing incrementally in charge and multiplicity, (ii) accurately reproducing experimentally measured photoluminescence peaks, and (iii) energy-ordering defects of different types occurring within a given polytype. The extensibility of this approach to transition-metal defects is also tested by applying it to silicon-substituted chromium defects in SiC and comparing with measurements. It is demonstrated that, when used in conjunction with SIMOMM-optimized geometries, EOMCC-based methods can provide a reliable prediction of the ground-state charge and multiplicity, while also giving a quantitative description of the photoluminescence spectra, accurate to within 0.1 eV of measurement for all cases considered.

## **Observations of Anisotropic Oxide Growth in the Initial Oxidation of Ni-Base Alloys**

*E. Zeitchick<sup>1</sup> and J.H. Perepezko<sup>1</sup>*

<sup>1</sup>Department of Materials Science and Engineering, University of Wisconsin-Madison

The oxidation of Ni-base alloys has been a topic of considerable interest due to the impressive high temperature oxidation resistance of these alloys. The oxidation resistance of these alloys is reliant upon their ability to develop and maintain a continuous, dense, and slow-growing oxide scale on their surface, best accomplished by  $\text{Cr}_2\text{O}_3$  or  $\alpha\text{-Al}_2\text{O}_3$ . The formation of a complete, passivating oxide scale is preceded by an initial period of transient oxidation, where several oxide species can develop simultaneously, including  $\text{NiO}$ ,  $\text{Cr}_2\text{O}_3$ ,  $\text{NiCr}_2\text{O}_4$ ,  $\text{NiAl}_2\text{O}_4$ , and/or other polymorphs of  $\text{Al}_2\text{O}_3$ . Generally, the formation of non-passivating oxides is detrimental to the oxidation resistance of the alloy [1]. Studying the transient oxidation stage, and the associated anisotropic oxide growth, would allow better understanding of oxidation mechanisms so that the behavior of the system can be controlled for enhanced corrosion resistance.

[1] Young, J., *High Temperature Oxidation and Corrosion of Metals*, Elsevier, (2008), p.315-360.

## Modeling Electrochemical Oxide Growth Below the Debye Length

*R. Ramanathan<sup>1</sup> and P.W. Voorhees<sup>1</sup>*

<sup>1</sup>Department of Materials Science and Engineering, Northwestern University

Understanding the growth of a passive oxide film in aqueous environments requires a description of the strong coupling between the electrostatic potential and defect transport in the film. Most oxide growth models, such as MacDonald's Point Defect Model (PDM) [1], consider the potential drop through the film to be linear, and thus implicitly assume that the film is uncharged. This assumption is likely to be violated for films whose thicknesses are of the same order of magnitude as the Debye length in the film. In these cases, alternative models must be used that solve Poisson's equation for the electrostatic potential.

As a first attempt, we have developed a modified PDM for the growth of thick, uncharged films. Our model solves Laplace's equation for the potential and accounts for the Helmholtz double layer in the electrolyte. By ensuring that Gauss's law is satisfied at the oxide/electrolyte interface, we can describe how the potential drop evolves at that interface as the film grows. We assume that the growth of the film occurs through anion vacancy transport, and include the PDM's description of film dissolution so that the model can describe a steady-state film thickness. The modified PDM successfully reproduces the observed variation of the steady-state film thickness with anode voltage and solution pH. We perform a linear perturbation analysis of the model to find out if deviations from planarity of the oxide/electrolyte interface are unstable.

[1] D.D. MacDonald and M. Urquidi-MacDonald, Theory of steady-state passive films, *J. Electrochem. Soc.*, **137**(8) (1990) 2395-2402.

## **Phase Field Modeling of Oxide Growth**

*K. Kim<sup>1</sup> and P.W. Voorhees<sup>1</sup>*

<sup>1</sup>Department of Materials Science and Engineering, Northwestern University

A phase-field model of an oxide relevant to corrosion resistant alloys for film thicknesses below the Debye length  $LD$ , where charge neutrality in the oxide does not occur, is formulated. The phase-field model is validated in the Wagner limit using a sharp interface Gouy-Chapman model for the electrostatic double layer. The phase-field simulations show that equilibrium oxide films below the Wagner limit are charged throughout due to their inability to electrostatically screen charge over the length of the film,  $L$ . The character of the defect and charge distribution profiles in the oxide vary depending on whether reduced oxygen adatoms are present on the gas-oxide interface. The Fermi level in the oxide increases for thinner films, approaching the Fermi level of the metal in the limit  $L/LD \rightarrow 0$ , which increases the driving force for adsorbed oxygen reduction at the gas-oxide interface.

## **Pourbaix diagrams for transition metals and their alloys**

*L.F. Huang<sup>1</sup>, M.J. Hutchinson<sup>2</sup>, R.J. Santucci<sup>2</sup>, J.R. Scully<sup>2</sup>, and J.M. Rondinelli<sup>1</sup>*

<sup>1</sup>Department of Materials Science and Engineering, Northwestern University

<sup>2</sup>Department of Materials Science and Engineering, University of Virginia

Magnetic transition metals ( $m\text{TM}$  = Cr, Mn, Fe, Co, and Ni) and their complex compounds (e.g., oxides, hydroxides, and oxyhydroxides) are highly important technology-relevant materials. The corrosion and oxidation resistances of these materials at variable electrochemical conditions are critical factors for their design, synthesis, and application, and can be effectively predicted using phase diagrams with respect to electrode potential and solution pH, i.e., Pourbaix diagram. However, the structures and free energies of formation ( $\Delta fG$ ) required in the modeling the Pourbaix diagram are frequently inaccurate or even absent from existing experimental databases, resulting in some Pourbaix diagrams inconsistent with direct electrochemical observations. In this work, we propose a high-throughput method based on density-functional theory (DFT), which screens out the ground-state structures for  $m\text{TM}$  compounds using efficient DFT methods, to obtain accurate  $\Delta fG$ 's using high-level DFT methods, followed by the phase-diagram construction with these calculated free energies of formation as input. We show the new Pourbaix diagrams from DFT are consistent with various electrochemical observations, and systematically exhibit higher reliability than the previous ones. We further use the accurate  $\Delta fG$ 's for Ni- and Cr-based oxides in modelling the Pourbaix diagrams of Ni-Cr alloys, which helps us understand their composition-dependent oxidation and corrosion behaviors.

## **In-situ observations on early stage oxidations of Ni-Cr and Ni-Cr-Mo alloys**

X.X. Yu<sup>1</sup>, A. Gulec<sup>1</sup>, C. Andolina<sup>2</sup>, J. Yang<sup>2</sup>, and L.D. Marks<sup>1</sup>

<sup>1</sup>Department of Materials Science and Engineering, Northwestern University

<sup>2</sup>Department of Chemical and Petroleum Engineering, University of Pittsburgh

By *in-situ* TEM experiments on the early stage oxidations of Ni-Cr and Ni-Cr-Mo alloys, it is found that the NiO will firstly initiate and epitaxially grow on the surface of both alloys by layer-by-layer mode. For NiCr alloys, a sequence oxide initiation and phase separation:  $\text{NiO} \rightarrow \text{NiCr}_2\text{O}_3 \rightarrow \text{Cr}_2\text{O}_3$  has been observed, however, for NiCrMo alloys, the metal-stable  $\text{Ni}_{2-x}\text{Cr}_x\text{O}_3$  (corundum structure) phase formed shortly after the growth of NiO. The results show the oxidization mechanism at the atomic level and reveal the possible molybdenum effect to increase the oxidation resistance to Ni-based alloys.

The authors gratefully acknowledge funding from the Office of Naval Research MURI “Understanding Atomic Scale Structure in Four Dimension to Design and Control Corrosion Resistant Alloys” on Grant number N00014-16-1-2280.

## **TEM investigation on pulse oxidation of NiCr alloys**

*X.X. Yu<sup>1</sup>, E. Zeitchick<sup>2</sup>, J. Perepezko<sup>2</sup> and L.D. Marks<sup>1</sup>*

<sup>1</sup>Department of Materials Science and Engineering, Northwestern University

<sup>2</sup>Department of Materials Science and Engineering, University of Wisconsin–Madison

NiCr alloys with Cr content varying from 1 at% to 32.6 at% by pulse oxidation were investigated by electron microscopy. Cr enrichment was found during the oxidation, however, the Cr distribution changed with the Cr content in the alloys. Cr was rich at metal/oxide interface in Ni-1Cr. Cr trapped in the rocksalt Ni oxide was found in Ni-5Cr. The separation of NiO and Cr<sub>2</sub>O<sub>3</sub> phases from the solute trapped rocksalt structure has been found in Ni-30Cr. Collective results show the possible path way of thermodynamic stable oxides phases growth from the solute trapping region at metal/oxide interface.

The authors gratefully acknowledge funding from the Office of Naval Research MURI “Understanding Atomic Scale Structure in Four Dimension to Design and Control Corrosion Resistant Alloys” on Grant number N00014-16-1-2280.

## Flexoelectric Effects in Single Crystals

*C. Mizzi<sup>1</sup>, P. Koirala<sup>1</sup>, E. Guo<sup>1</sup>, and L.D. Marks<sup>1</sup>*

<sup>1</sup>Department of Materials Science and Engineering, Northwestern University

Although first proposed in 1964 [1] and first observed in 1968 [2], flexoelectricity, the electromechanical coupling between polarization and strain gradient, in crystalline solids has remained largely unexplored. However, a number of experiments in the early 2000s helped to establish the flexoelectric effect as an important phenomenon in a large number of complex oxides, especially at the nanoscale [3]. Since applying a strain gradient is inherently symmetry breaking, flexoelectricity can be found in both centrosymmetric and non-centrosymmetric materials. This has generated interest in utilizing flexoelectricity in applications that have traditionally relied upon piezoelectricity and a number of demonstrations have already shown the feasibility of flexoelectric devices [4].

We report flexoelectric characterization across a wide range of bulk single crystals performed with a three-point bending method [5]. Our studies of magnesium oxide, lanthanum aluminate, niobium-doped strontium titanate and lanthanide scandates indicate that many materials defy conventional flexoelectric theory which posits that flexoelectricity scales with dielectric constant and begs to question: what is the cause of a large flexoelectric response. To this end, the microstructural and electronic origins of flexoelectric enhancements and the implications of these results in the context of thin film growth are explored.

- [1] S. M. Kogan, Piezoelectric effect during inhomogeneous deformation and acoustic scattering of carriers in crystals, *Sov. Phys. Solid State* 5 (1964) 2069-2070.
- [2] E. V. Bursian and O. I. Zaikovskii, Changes in the curvature of a ferroelectric film due to polarization, *Sov. Phys. Solid State* 10 (1968) 1121-1124.
- [3] P. Zubko, G. Catalan, and A. K. Tagantsev, Flexoelectric Effect in Solids, *Annu. Rev. Mater. Res.* 43 (2013) 387-421. DOI: 10.1146/annurev-matsci-071312-121634
- [4] U. K. Bhaskar, N. Banerjee, A. Abdollahi, Z. Wang, D. G. Schlom, G. Rijnders, and G. Catalan, A flexoelectric micromechanical system on silicon, *Nat. Nanotechnol.* 11 (2016) 263-266. DOI: 10.1038/nnano.2015.260
- [5] P. Koirala, C. Mizzi, and L. D. Marks, Direct Observation of Large Flexoelectric Bending at the Nanoscale in Lanthanide Scandates, *arXiv:1511.07791* (2016).

This work was supported by the Department of Energy on Grant Number DE-FG02-01ER45945.



## **Grain Boundary Assisted Crevice Corrosion in CoCrMo Alloys**

*A. Lin<sup>1</sup>, E.E. Hoffman<sup>1</sup>, and L.D. Marks<sup>1</sup>*

<sup>1</sup>Department of Materials Science and Engineering, Northwestern University

Cobalt-chromium-molybdenum (CoCrMo) alloys have been extensively used for biomedical implants, but are susceptible to grain boundary corrosion due to local chromium depletion, commonly referred to as sensitization. In this work, selected boundaries from electrochemically corroded CoCrMo alloys were analyzed from the millimeter to the nanometer scale in order to link the chemical composition and coincident site lattice geometries to the observed local corrosion behavior. Grain boundaries of varying degrees of misorientation were examined by optical profilometry and transmission electron microscopy, and grain boundary precipitates were analyzed with energy dispersive X-ray spectroscopy. Low- $\Sigma$  coincident site lattice boundaries were found to have fewer carbide precipitates and smaller degrees of sensitization and are more resistant to intergranular attack. Similar to general high-angle boundaries, the combination of chromium depletion and the grain boundary interfacial energy acts as the initiator of corrosion. After initiation, crevice corrosion continues to enlarge the initial site of the attack. The model presented can be used to refine the processing procedures of CoCrMo alloys and other alloys for enhanced corrosion resistance.

[1] E. E. Hoffman, A. Lin, Y. Liao, L.D. Marks. *Corrosion*, 2016; 72(11), 1445-1461.

[2] A. Lin, E. E. Hoffman, L.D. Marks. *Corrosion*, 2017; 73(3), 256-267.

This research was funded by the National Science Foundation on grant number CMMI-1030703. AL was assisted by grants from the Undergraduate Research Grant Program which is administered by Northwestern University's Office of Undergraduate Research. EEH was supported by the Department of Defense (DoD) through the National Defense Science and Engineering Graduate Fellowship (NDSEG) program.

## **NiCrMo Oxidation Revealed by Cryo-Electron Microscopy**

*A. Lin<sup>1</sup>, A. Mueller<sup>2</sup>, A. Minor<sup>2,3</sup>, and L.D. Marks<sup>1</sup>*

<sup>1</sup>Department of Materials Science and Engineering, Northwestern University

<sup>2</sup>National Center for Electron Microscopy, Molecular Foundry, Lawrence Berkeley National Laboratory

<sup>3</sup>Department of Materials Science and Engineering, University of California, Berkeley

Hydroxide and chloride ion concentrations at the oxide edge and in the oxide are critical for understanding early-stage oxidation across many corrosion-resistant alloys. Additionally, further characterization of oxide structure, composition, and defects is vital for developing more accurate models for oxide growth and breakdown. Observing oxide growth and breakdown during aqueous corrosion presents significant challenges. Many of the hydroxides and chlorides trapped in the oxide are unstable in an ambient environment and beam-sensitive, limiting the use of conventional transmission electron microscopy (TEM) for these solid-liquid interfaces. In order to avoid sample dehydration, corroded NiCrMo alloys were cryo-immobilized by rapid freezing. A cryo-focused ion beam was used to polish the alloy to electron transparency, while preserving the alloy-water interface, and the sample was then cryo-transferred to a TEM for imaging and energy dispersive X-ray spectroscopy. The presence of rocksalt, corundum, and  $\beta$ -Ni(OH)<sub>2</sub> phases was confirmed with electron diffraction.

The authors gratefully acknowledge funding from the Office of Naval Research MURI “Understanding Atomic Scale Structure in Four Dimension to Design and Control Corrosion Resistant Alloys” on Grant number N00014-16-1-2280. Work at the Molecular Foundry was supported by the Office of Science, Office of Basic Energy Sciences, of the US Department of Energy under Contract number DE-AC02-05CH11231.

## **Correlation Between Electrochemical Behavior and Nanoscale Characterization of Single Grains of Ni-Cr and Ni-Cr-Mo alloys**

*K. Gusieva<sup>1</sup>, K. Lutton<sup>1</sup>, W. Blades<sup>1</sup>, C. Volders<sup>1</sup>, G. Ramalingam<sup>1</sup>, E. Zeitchick<sup>2</sup>, J. Perepezko<sup>2</sup>, P. Reinke<sup>1</sup>, and J. Scully<sup>1</sup>*

<sup>1</sup>Department of Materials Science and Engineering, University of Virginia

<sup>2</sup>Department of Materials Science and Engineering, University of Wisconsin-Madison

The effect of crystal orientation and prior etching on the electrochemical polarization behavior and repassivation kinetics of Ni-Cr and Ni-Cr-Mo alloys during potential step polarization into the passive range has been investigated. We apply a combination of electrochemical methods with real time monitoring of global and local, single grain measurements. The passivation is investigated in an acidic chloride environment using single frequency electrochemical impedance spectroscopy in the passive region of the alloys at potentials where breakdown is possible. This is one of the few studies where single grain performance is monitored in an electrochemical process, and illuminates the critical impact of orientation on passivation behavior. It paves the path to future work combining surface morphology analysis with electrochemistry and passivation analysis, and develops a more accurate understanding and interpretation of the passivation mechanism of Ni-Cr and Ni-Cr-Mo alloys.

## **Initial Stages in the Pesting and Passivation of Mo-Silicides Observed at the Nanoscale**

*C. Volders<sup>1</sup> and P. Reinke<sup>1</sup>*

<sup>1</sup>Department of Materials Science and Engineering, University of Virginia

The use of Mo-silicides in technical applications depends on their unique resistance to corrosion once the formation of a SiO<sub>2</sub> scale has been achieved. At lower temperatures the oxidation process is destructive a pesting reaction leads to rapid disintegration of the material. The interplay between mixed oxide formation in the pesting regime and the transition out of this regime to SiO<sub>2</sub> scale formation due to the volatilization of MoO<sub>3</sub> govern the oxidation of MoSi<sub>2</sub> prior to protective silica formation. This work presents a study of the oxidation of nanometer-scale MoSi<sub>2</sub> crystallites with the use of Scanning Tunneling Microscopy/Spectroscopy (STM/STS). Oxidation is initiated by a nascent period with subtle modulations of the surface electronic structure due to oxygen adsorption. This is followed by a rapid onset of pesting recognized by a dramatic increase in crystallite density. The O-adsorption destabilizes the silicide surface and opens reaction pathways to MoO<sub>x</sub> formation – or vice versa – O-adsorption stabilizes the surface at a temperature where thermodynamics already favors MoO<sub>x</sub> formation. Pesting is a non-local reaction and diffusion of MoO<sub>x</sub> drives the rapid spread of the destructive reaction. This is followed by transition to SiO<sub>2</sub> for T>750°C. Direct observation of pesting can be combined with DFT modeling of surface reactions, and contribute to develop and understand strategies to mitigate pesting and advance scale formation.

## **From Alloy to Oxide: Nanoscale View of NiCr Oxidation for Ni 5Cr to Ni 30Cr**

*W. Blades<sup>1</sup>, G. Ramalingam<sup>1</sup>, R. Ramanathan<sup>2</sup>, P.W. Voorhees<sup>2</sup>, J. Rondinelli<sup>2</sup>, and P. Reinke<sup>1</sup>*

<sup>1</sup>Department of Materials Science and Engineering, University of Virginia

<sup>2</sup>Department of Materials Science and Engineering, Northwestern University

The initial steps of alloy oxidation are studied with atomic resolution in geometric and electronic structure with STM and STS. The oxidation of Ni (100) surfaces is kinetically hindered by step edge straightening forced by the Ni(100)-c(2x2) reconstruction. This nucleation barrier is lifted and the kinked step edges are again available for nucleation. Ni nCr(100) alloys therefore show a much more rapid oxidation. Modeling of oxide island growth in conjunction with statistical analysis of island density, height and size, yields a capture radius for O of only a few interatomic distances and island growth progresses via the island perimeter. At elevated temperatures 500° - 600°C the difference between pure Ni and Ni nCr is even more pronounced and rapid nucleation of NiO at step edges initiates the oxide layer growth. The local measurement of the Fermi energy position within the NiO gap with STS illustrates the variations in electronic structure, which are subsequently expected to impact the development of the Mott potential. Cr acts for the (100) surface as a catalyst to NiO nucleation albeit the details of the underlying mechanism are not yet fully understood. In the context of other work presented here it is evident that crystallographic orientation impacts the surface chemistry critical to oxidation. We will design experiments which focus on the role of individual dopant atoms introduced in a controlled manner during the oxidation process.

## **Surface Reactions and Kinetics in Ni-Cr Alloy Oxidation and the Role of a Third Alloying Element (Mo, W)**

*C. Volders<sup>1</sup>, V. Avincola<sup>1</sup>, E. Zeitchick<sup>2</sup>, J. Perepezko<sup>2</sup>, P.W. Voorhees<sup>3</sup>, and P. Reinke<sup>1</sup>*

<sup>1</sup>Department of Materials Science and Engineering, University of Virginia

<sup>2</sup>Department of Materials Science and Engineering, University of Wisconsin-Madison

<sup>3</sup>Department of Materials Science and Engineering, Northwestern University

The initial stages of oxidation (Mott-Cabrera regime), when the first few nanometers of oxide are formed, were studied with ambient pressure-XPS in real time at  $p(\text{O}_2)$  0.01 to  $10^{-6}$  mbar and temperatures from 300 to 500°C during oxidation. Alloy compositions are Ni 5at%Cr (Ni 5Cr) and Ni 15Cr, and Ni 30Cr, as well as Ni 15Cr 6W and Ni 15Cr 6Mo to study the impact of a third alloying element. In contrast to our STM work, this set of experiments uses cast alloys with a wide range of surface orientations. The alloy surfaces are Cr-enriched, and rapid chromia formation ensues, followed by slower growth of NiO. The oxide-oxygen/vacuum interface is O-terminated with an adsorbed oxygen layer. The Cr-supply from the alloy is limited and stunts Cr-oxide growth with NiO taking over at about 3-4 nm oxide thickness. The double-layer oxide structure has to be considered in the discussion of the overall Mott potential. W in general suppresses NiO and favors Cr-oxide growth with W(Mo) oxides accumulating preferentially at the oxide-alloy interface, albeit the magnitude of this effect appears to be strongly orientation dependent leading to sample-to-sample variations. The Mott potential measured as the built-in potential with XPS across the oxide layer is about 0.3 eV. The consequences of sample inhomogeneity caused by solute trapping, doping, and oxide-oxide interfaces, and the details of kinetics and bonding will be discussed.

## **Stable MoSi<sub>2</sub> nanofilms with controllable and high metallicity**

*L.F. Huang<sup>1</sup>, C. Volders<sup>2</sup>, G. Ramalingam<sup>2</sup>, P. Reinke<sup>2</sup>, and J.M. Rondinelli<sup>1</sup>*

<sup>1</sup>Department of Materials Science and Engineering, Northwestern University

<sup>2</sup>Department of Materials Science and Engineering, University of Virginia

Mo-Si structural alloys are promising for various ultrahigh-temperature applications owing to their excellent thermomechanical properties. Having an outstanding oxidation resistance, the native silicide MoSi<sub>2</sub> is used as a coating to protect Mo-Si alloys. In this work, using density-functional theory (DFT) calculations, we propose an alternative novel use of MoSi<sub>2</sub> nanofilms for electronics. The favorable thermodynamic and dynamical stabilities of MoSi<sub>2</sub> nanofilms are comprehensively assessed using their formation energies, phonon spectra, and surface energies, which indicate their facile synthesis in experiment. We find that the metallicity of the MoSi<sub>2</sub> nanofilms are sensitive to the nanofilm type (crystal structure) and thickness. We explain how these dependencies arise from quantum-confinement and surface effects. The high and tunable metallicity of MoSi<sub>2</sub> nanofilms found here may be used in a variety of architectures employing two-dimensional materials and functional oxides, and our reported electronic mechanism may be helpful for understanding and improving the oxidation resistance of MoSi<sub>2</sub> alloy.

## Surface Oxidation of Metal Nanoparticles

A. Yoon<sup>1,2</sup>, and J.M. Zuo<sup>1,2</sup>

<sup>1</sup>Materials Science and Engineering, University of Illinois at Urbana Champaign

<sup>2</sup>Fredrick Seitz Material Research Laboratory, University of Illinois at Urbana Champaign

Metal nanoparticles (NPs) are extensively employed in a broad range of applications in chemical industry, energy conversion and environmental remediation. The surface of NPs differs from the 2D bulk surface because of their smaller size and 3D shape. How the 3D shape of NPs impact on the oxide formation, however, is not clear. Here, we demonstrate the shape changes of Pd nanocrystals and their surface structure upon oxidation based on the observations carried out in an environmental transmission electron microscope (ETEM). The palladium nanocrystals were prepared on an oxide powder support using an e-beam evaporator and were annealed at 300 °C to form equilibrium shapes before oxidation. Oxidation was done inside the ETEM at 300-400 °C with  $2 \times 10^{-5}$  mbar of oxygen pressure. Our results show that palladium nanocrystals undergo reversible shape changes. The equilibrium shapes of nanocrystals are truncated octahedron in vacuum, but become rounded when exposed to oxygen. The sharp edges of the truncated octahedron, formed by the intersection of  $\{111\}$  facets, are smoothed by the introduction of the new  $\{110\}$  planes. The appearance of the  $\{110\}$  plane at oxygen pressures is thus a clear evidence for the surface energy change among the available crystal planes. In addition to the shape change of the nanocrystals, we also observed surface modifications of the palladium nanocrystals with changing pressure. The complex oxide structure was formed on the surface of the nanocrystal and did not correspond to any stable phase of the bulk Pd oxide or the surface oxide found at the 2D bulk surface. This new oxide phase is suspected to be formed kinetically by the strong metal support interaction. Further investigation of the new surface phases and their thermodynamic validation will provide significant insights into surface oxidation of supported metal nanoparticles.

The ETEM is supported by DMR 12-29454. JMZ and AY are partially supported by DMR 14-10596, and AY is additionally supported by Kwanjeong Educational Foundation

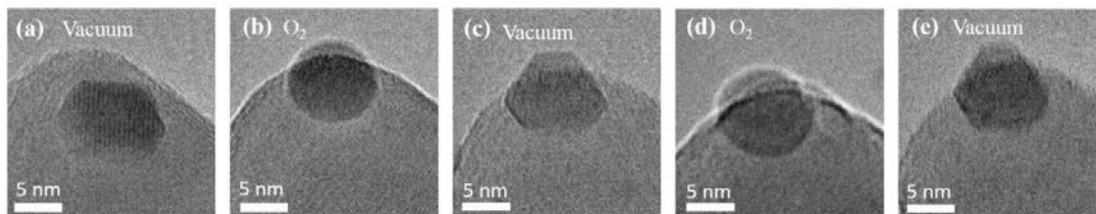


**Figure 1.** The shapes of a Pd nanocrystal observed on the TiO<sub>2</sub> nanoparticle support. The shape changed responding to the gas pressure changes. The truncated octahedral shape observed under vacuum became rounded after introducing oxygen. The shape change was reversible during the purging/introduction of oxygen gas. The vacuum here is the TEM base pressure of  $10^{-7}$  mbar in (a), (c) and (e), and O<sub>2</sub> in (b) and (d) is at the oxygen pressure of  $2 \times 10^{-5}$  mbar after O<sub>2</sub> gas injection.



## Constructing a Predictive Model of Copper Oxidation from Experiment and Theory

C.M. Andolina<sup>1</sup>, M.T. Curnan<sup>1</sup>, Q. Zhu<sup>1</sup>, W.A. Saidi<sup>2</sup>, and J.C. Yang<sup>1,3</sup>

<sup>1</sup>Department of Chemical and Petroleum Engineering, University of Pittsburgh

<sup>2</sup>Department of Mechanical Engineering & Materials Science, University of Pittsburgh

<sup>3</sup>Department of Physics and Astronomy, University of Pittsburgh

This work aims to establish a correlative investigation utilizing theory and *in situ* Environmental Transmission Electron Microscopy (ETEM) in tandem to bridge the spatial and temporal gaps between experimental and computational approaches. Initially focusing on the oxidation of copper (a well-studied model system for metal oxidation) [1], ultimately this work aspires to develop a continuous and precise predictive model of oxidation across all studied scales of measurement. We investigated the Cu<sub>2</sub>O island nucleation preference sites (edge or terrace) using both experiment and theory for three low index ((001), (011), and (111)) copper film surfaces. Initiation of controlled oxidation (O<sub>2</sub>) in situ was achieved using a custom built gas delivery system with three gas input lines a variety of available gases (CH<sub>4</sub>, CO<sub>2</sub>, CO, H<sub>2</sub>, H<sub>2</sub>O, Methanol, and O<sub>2</sub>). Computational methods, such as climbing image nudged elastic band within density functional theory (NEB-DFT) and molecular mechanics frameworks provided a quantitative and comprehensive assessment of the relative energetics of oxygen adsorption states, activation barriers, and surface reconstructions for different facets. [2,3] The most probable diffusion pathways of oxygen and adsorption sites predict whether nucleation of Cu<sub>2</sub>O is preferred at edge or terrace sites for given surface orientations. Cu<sub>2</sub>O island nucleation favors edge over terrace sites with increasing preference for Cu (001) compared to the Cu (011) and (111). Correlating these experimental data and simulations will reveal further relationships between reaction mechanisms and aid in developing a holistic understanding of how oxidation proceeds. This, in turn, will enhance the predictive power of computational models of oxidation onset [4,5], and ultimately direct future corrosion mitigation strategies, as well as the engineering of materials tuned for specific applications. [6]

[1] Q Zhu, et al. *Surface Science* **652** (2016), p. 98.

[2] G. Henkelman, et al. *Journal of Chemical Physics* **113** (2000), p.9901.

[3] Q. Zhu, et al. *Journal of Physical Chemistry Letters* **7** (2016), p.2530.

[4] G. Zhou, et al. *Physical Review Letters* **109** (2012), p.235502.

[5] Q. Zhu, et al. *Journal of Physical Chemistry C* **119** (2015), p.251.

[6] The authors acknowledge National Science Foundation funding, Division of Materials Research, Grants #1508417 and 1410055. The Petersen Institute for NanoScience and Engineering Nanoscale Fabrication and Characterization Facility: Mr. Matt France and Dr. Susheng Tan.